SAND2017-4965C

Energy Harvesting for Increased Safeguards Equipment Battery Life

Ross Hymel

Sandia National Laboratories (SNL)
PO Box 5800, Albuquerque, NM USA 87185-1373
E-mail: rwhymel@sandia.gov

Abstract:

Most unattended safeguards equipment (e.g. electronic seals) use some form of battery—traditionally an expensive, bulky and, oftentimes, hazardous lithium battery. The limited charge-life of these batteries necessitates periodically replacing them or the equipment they power (if batteries are not field-replaceable) to prevent total battery discharge and potential loss of continuity of knowledge. These maintenance cycles present a significant monetary cost to a safeguards inspectorate and demand on in-field inspector time, as well a potential increase in personnel exposure to damaging radiation.

One approach to increasing the operational lifetime of this equipment is known as energy harvesting: the process by which energy is replenished by collection and storage from external source(s). The replenished, stored energy can be used to supplement the energy available from the initial battery charge. This paper examines energy harvesting via photovoltaic (PV) cells, both monocrystalline and amorphous, and the cells' associated performance across the entire infrared to UV spectrum, including both indoor and outdoor lighting conditions. It then explores the system architecture required for energy harvesting as well as the design trade-offs available. Finally, this paper assesses the performance of a prototype system incorporating this type of energy harvesting in a real-world application.

Keywords: safeguards, containment, batteries, energy harvesting

1. Introduction

Modern unattended safeguards equipment (e.g. seals) incorporates many low-power electronic circuits, which are typically powered by expensive and toxic lithium thionyl chloride ($LiSOCL_2$) batteries. The limited life of these batteries necessitates their periodic replacement. This replacement must be performed before total battery discharge to avoid potential loss of continuity of knowledge. Thus, the effective battery capacity becomes significantly less than the actual usable capacity. Additionally, such maintenance is a radiological hazard to personnel, as well as a monetary burden to a safeguards inspectorate.

Energy harvesting, a commercially available technology, could extend the operational life of battery-powered equipment to achieve significant efficiencies for safeguards deployments. Energy harvesting is the scavenging and storage of ambient energy sources, such as solar, thermal, and kinetic for use in low-power electronic applications. While the amount of scavenged energy per unit time may be small, it most often comes from a source that will not be depleted throughout the deployment of the harvesting device. The best-known energy harvesters are solar panels and wind turbines.

Recently, far-field wireless energy harvesting has become a commercially available option. Far-field wireless energy harvesting provides consistent, predictable, and un-tethered power over distances up to 50 feet. This process converts radio frequency (RF) energy, both intentionally emitted and ambient, into usable direct current (DC) power. Incorporating far-field wireless energy harvesting into safeguards equipment can significantly extend the equipment's battery life and perhaps make it indefinite. Furthermore, additional functionality can be added to safeguards equipment without lowering its operational life expectancy. This type of energy harvesting was previously explored, and the results can be found here [1].

Alternatively, should RF harvesting not be permitted or desired, photovoltaic-based harvesting is a promising substitute. Photovoltaic (PV) cells are semiconductor devices that convert incident photons directly into electricity via the photovoltaic effect. These cells come in several types depending on the underlying crystalline structure and include amorphous, polycrystalline, and monocrystalline. Recent advances in monocrystalline panel technology enable such cells to convert up to 22% of ambient light energy into usable electric power. Should cost be the overriding factor, cheaper, but less efficient, amorphous cells are also an option.

This paper explores the benefits and drawbacks of integrating energy harvesting into a chosen safeguards seal: the Remotely Monitored Sealing Array (RMSA). Specifically, it examines the usage of commercially-available PV cells, amorphous and monocrystalline, detailing the pros and cons of each type as well as the in-system performance.

2. Photovoltaic energy harvesting overview

Figure 1 shows a high-level diagram of a PV-based energy harvesting system.

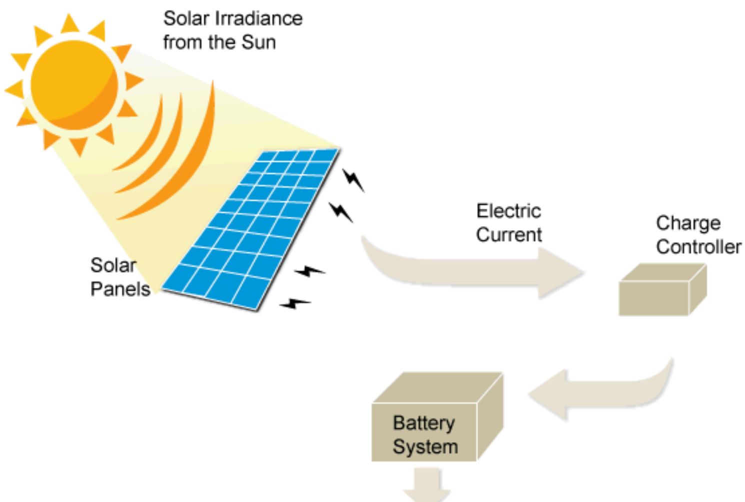

Figure 1: PV-based Energy Harvesting System (image courtesy http://lifefreeenergy.com)

Such a harvesting solution typically contains four main blocks. First, a source of photonic energy, such as the sun, must be available. While solar irradiance is the preferred form of energy, providing up to an order of magnitude more photonic energy than indoor lighting, the system itself is only weakly constrained to the form and strength of lighting. Certain cells are optimized for operation under specific light intensities, for example indoor cells that must not experience greater than 1000 lux illumination. Also, all cells have a varying efficiency across wavelength and will produce a larger signal output based on the spectral content of the lighting source. This non-ideal behaviour is known as external quantum efficiency and will be discussed later.

Next, a small PV cell must be exposed to this lighting. When irradiated, a PV cell behaves analogously to a current source. As irradiation increases, so too does the amount of charge available for collection. Such cells are self-limiting; as the attached electronic load increases, the output voltage of the cell drops, finally reaching its short circuit current (I_{SC}) at a zero ohm load. Similarly, as electronic load decreases, the output voltage of the cell rises, eventually reaches its open circuit voltage (V_{OC}). All points in between are characterizable and form the cell's I-V curve. Figure 2 displays an example I-V curve for an IXYS brand solar cell. The blue line plots the cell's voltage and current under fixed lighting conditions but with an electronic load that varies by small increments from 0 to ∞ ohms.

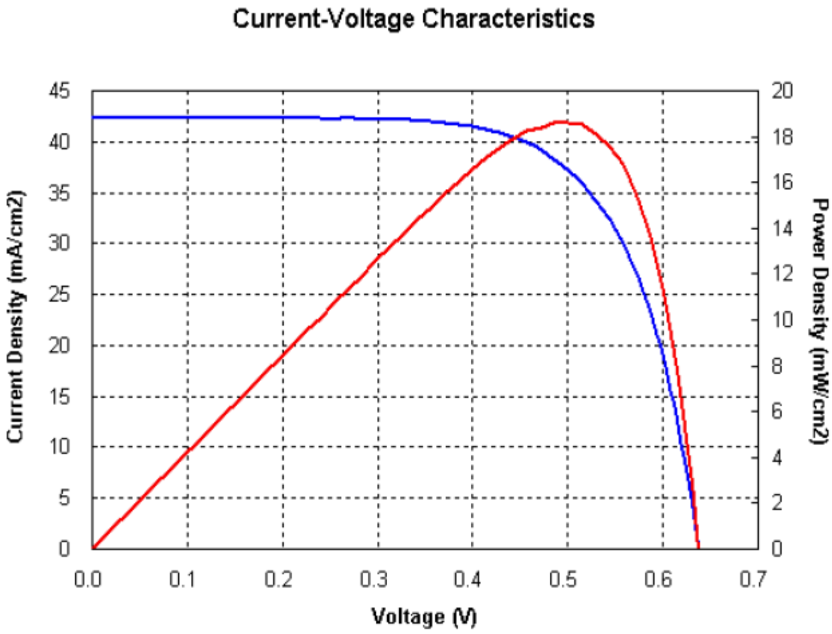

Figure 2: Representative I-V Curve (image courtesy http://ixys.com)

As can be seen, even under fixed illumination, the power available from the cell varies based on the electronic bias point of circuit. The red line plots the variation of power available from the cell under different loads. There is clearly a point of largest power, known as the maximum power point (MPP), and, for solar cells, it typically occurs at 80% of the open circuit voltage.

Because the energy delivered by the cell must be collected in a very specific manner to optimize the efficiency, a specialized circuit is needed that can properly bias the cell at its MPP as well as convert the low voltage energy into a more usable form. The charge controller in Figure 1 is this element. Even for indoor lighting, the illumination levels, and thus the charge generated by the cell, will vary significantly throughout the day. The charge controller must dynamically vary the impedance presented to the cell in order to maintain operation at the MPP. Further, most electronic systems require a constant, well-regulated voltage to operate correctly. The charge controller must also employ a voltage converter to transform the varying input voltage into a constant, predictable output voltage.

Lastly, solar cells are not able to store energy. Should the cell generate energy in excess of what is required for the load, this additional energy would be lost. While such an approach may be tolerable in a simple system where the lighting conditions are known and continuous, a more advanced system will employ some form of energy storage. This energy storage allows the system to continue to operate without depleting the primary batteries when the photonic source is removed, for example at night when the lights are turned off. Many different form of energy storage are available, including rechargeable batteries and supercapacitors. Each have different charging methods, such as constant current or constant voltage, and the previously mentioned charge controller must be able to provide the appropriate form. Also, each type of energy storage has different capacity, cost, and self-discharge, so care must be taken when down-selecting for an application.

2.1. PV cell evaluation

For this evaluation, three PV cells were evaluated, each cell having varying characteristics and use cases. Their measured parameters are listed in
Table 1. All cells were first tested using white light under 1.0 sun (1000 W/m^2). They were then retested using ambient room lighting (10 W/m^2). For each test, the load presented to the cell was varied such that the voltage across the cell increased in 0.01 V increments.

	AM-5902CAR	AM-1816CAR	SLMD121H10L
Crystal Type	Amorphous	Amorphous	Monocrystalline
Intended Use	Outdoor	Indoor	Dual
I_{SC} (1000 W/m^2)	58.6 mA	3.55 mA	35.7 mA
V_{OC}	7.86 V	6.24 V	6.64 V
P_{MAX}	254 mW	5.26 mW	173 mW
Fill Factor (FF)	0.550	0.00526	0.728
I_{SC} (10 W/m^2)	202 µA	227 µA	132 µA
V_{OC}	5.1 V	5.2 V	3.46 V
P_{MAX}	600 µW	770 µW	264 µW
Fill Factor (FF)	0.582	0.653	0.577
Size	8.72 in^2	8.50 in^2	2.28 in^2
Unit Cost (quantity 10)	$23.06	$9.56	$11.81

Table 1: Evaluated PV Cell Parameters (0.1 Sun)

I_{SC} is the current through the cell when the cell is shorted, i.e. the voltage across the cell is zero. This number represents the maximum amount of current the cell can deliver, and, for a cell with moderate resistivity, is relatively flat even as the voltage increases up to the MPP.

V_{OC} is the voltage across the cell when the cell is open circuited, i.e. the current through the cell is zero. This parameter will influence the choice of charge controller, as the value must not be so low that the charge controller fails to start-up and not so high that the charge controller is damaged. Please note that no power can be extracted from the cell in either I_{SC} or V_{OC} conditions.

P_{MAX} represents the maximum power the cell can deliver and is easily calculated by tracing the I-V curve and using the equation P = I*V. As previously mentioned, power will be zero at the I_{SC} and V_{OC} points, with maximum power occurring at some point in between, usually 80% of V_{OC}.

Fill factor (FF) measures the quality of a solar cell. An ideal solar cell's I-V curve is a flat square, with vertex at (I_{SC}, V_{OC}). For such a cell, $P_{MAX} = I_{SC} * V_{OC} = P_T$ (theoretical power) resulting in a FF of 1. Actual cells operate below this point due to losses such as internal resistance and diode effects. Fill factor is graphically represented in Figure 3, and is the ratio of P_T to P_{MAX}.

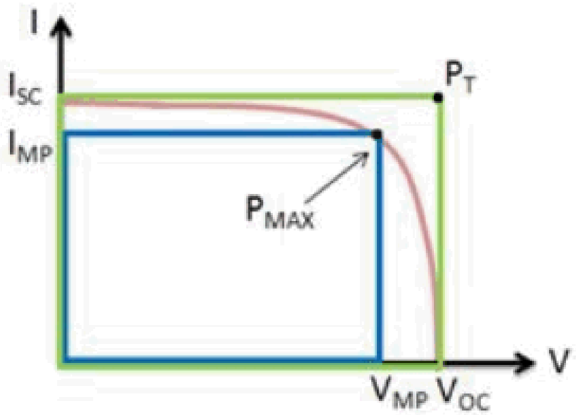

Figure 3: Graphical illustration of FF (image courtesy http://ni.com)

For all electrical parameters listed above (I_{SC}, V_{OC}, P_{MAX}, and FF), a higher number is better. However, size and cost must also be considered when selecting a cell. For both indoor and outdoor lighting conditions, the SLMD121H10L has the greatest electrical performance per square inch. If cost is the overriding factor, the SLMD121H10L should be used outdoors while the AM-1816CAR should be chosen for indoor applications.

The above measurements were all taken under uniform, white light conditions (400 nm to 700 nm). Realistic lighting conditions will not be evenly distributed across all spectral wavelengths. A measure of the cell's response versus frequency is known as the external quantum efficiency. This metric is the ratio of the number of charge carriers collected by the cell versus the number of photons incident on the cell. An ideal cell will have a quantum efficiency of 100% across all wavelengths. Actual cells will have optical losses due to recombination effects. Figure 4 plots the measured EQE of all three cells across the infrared (IR) (700 - 1100 nm) to ultraviolet (UV) (< 400 nm) spectrum in 10 nm increments.

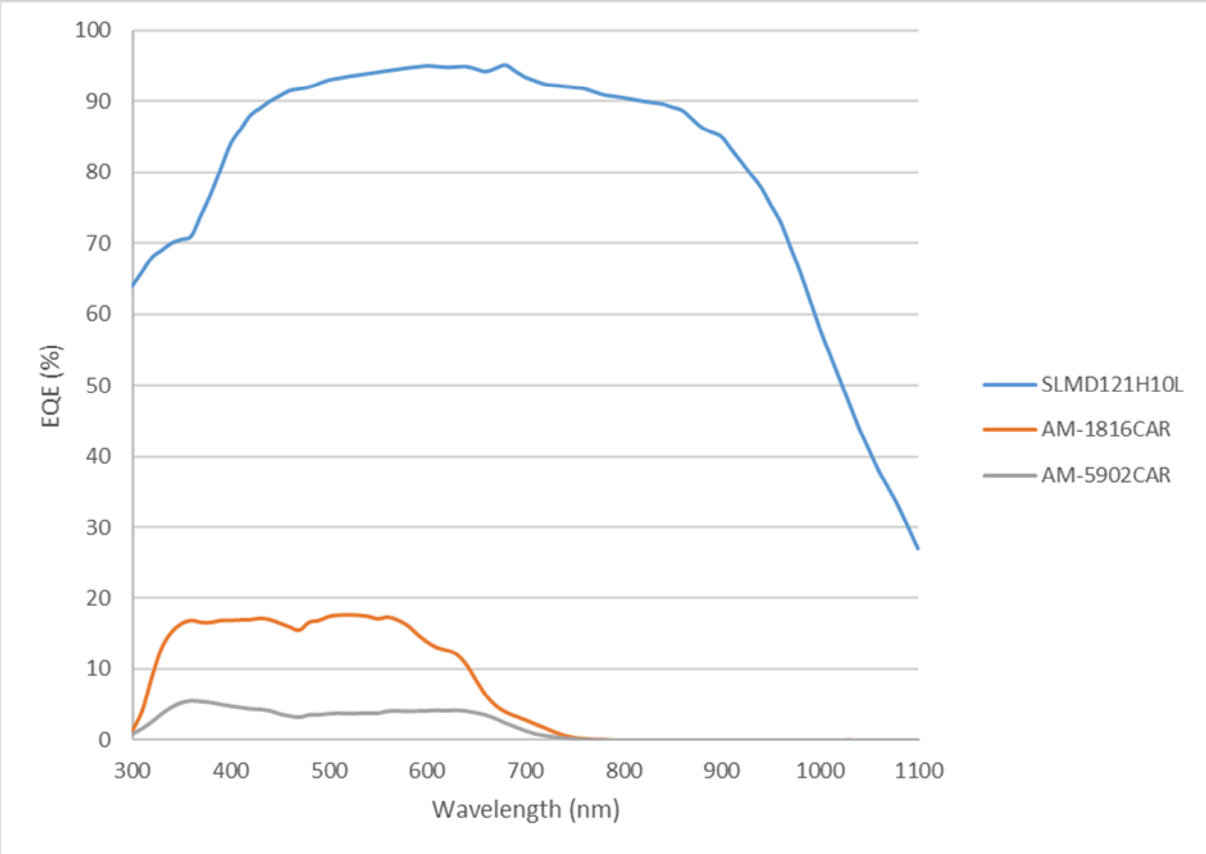

Figure 4: EQE measurements

Once again, the higher the external quantum efficiency the better. Here the advantages of monocrystalline cell construction are evident. The SLMD121H10L can operate across the entire spectral range, while the two amorphous cells are limited to the 300 nm to 600 nm visible portion. This larger area of operation will result in increased power conversion efficiency when operated in the presence of infrared and ultraviolet light, especially outdoors. Further, the quantum efficiency is significantly higher, allowing a much smaller cell to be used for similar energy harvesting results.

Lastly, monocrystalline cells have less temperature dependence than other types. In general, the voltage output of a cell will decrease with increasing temperature. While this effect occurs in monocrystalline cells, the net effect is less severe than in amorphous and polycrystalline cells. For the above tested cells, the monocrystalline will experience a -0.03 %/K degradation in V_{OC} while the amorphous cells will undergo -0.3 %/K, an order of magnitude increase.

3. Charge controller and energy storage

The circuit topology for collecting and storing charge generated by the solar cells can take on many different forms depending on the objectives of the system. The options include battery replacement, battery extension, and tiered architectures.

The first option is the complete removal of system batteries. By calculating the load requirements of the attached system over the course of a lighting cycle (usually one full day), the designer can size a PV cell arrangement such that it will provide enough harvested energy to fully power the system over the entire cycle, with enough margin for off-normal events, such as clouds. Unfortunately, this option is unusable in the schema, as batteries must always be present in a secure system such as a seal. Otherwise, an adversary could turn of the lights or cover the cells with opaque material to force the seal to power down.

The second option is to increase the lifetime of the primary batteries by only powering the system from them when the energy harvester is not available. This option necessitates the same load requirement analysis as the battery removal option, but, rather than eliminating the batteries, significantly increases the time period between battery replacements.

For this evaluation, a tiered architecture was chosen consisting of a primary battery, a secondary storage unit, and the energy harvester. During normal operation, solar energy is harvested and stored in the secondary storage unit. This unit must be carefully sized such that it can fully power the system during the course of the lighting cycle where no solar energy is present. On initial power-on, the attached load is powered by the primary battery. Once the harvester has fully charged the secondary storage, the charge controller switches the power source from the primary batteries to the secondary storage. The harvester will continue to replenish this secondary storage so long as solar power is available. If solar re-charging is not available, the system will continue to run from the secondary source until the attached load drains it below a specified threshold, at which point system power will revert back to the primary batteries. Figure 5 presents a simplified representation of the tiered architecture.

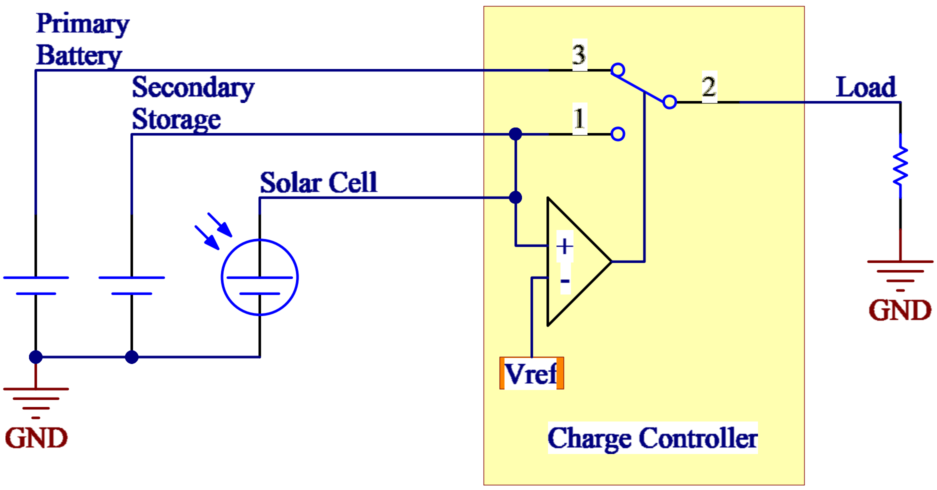

Figure 5: Tiered architecture block diagram

Besides being able to seamlessly switch between primary and secondary power (break-before-make), the charge controller must also be capable of several other important functions. These include:

- Programmable prevention of secondary storage over and under voltage to prevent damage
- Cold-start operation at extremely low levels of input voltage from the harvesting element (< 0.5 V) for start-up at low light levels
- Wide input voltage range (0.1 V to 5 V ideal) allowing for operation with many different kinds of PV cells

- Maximum power point tracking for optimal energy extraction
- Low quiescent current (< 1 μA ideal) to maximize energy delivery to the load

Several devices meet all these criteria, including the ADP5091 from Analog Devices, the SPV1050 from STMicroelectronics, and the BQ25505 from Texas Instruments. For this evaluation, the BQ25505 was chosen as it has the lowest quiescent current (325 nA typical) and start-up voltage (330 mV). These two parameters are most important, as they will minimize the drain on the primary batteries and allow for operation in very low lighting conditions. Additionally, the part has a wider input voltage and power range, allowing for use with most outdoor cells.

4. Seal Integration

To integrate PV energy harvesting into a safeguards seal such as RMSA, only minor modifications must take place. First, the PV cells must be mounted to the case and electrically connected to the base seal hardware. Because these cells require exposure to ambient light, they must be mounted externally. Luckily, existing RMSA cases already support both external and internal antenna configurations. Instead of installing an external antenna, the existing antenna connector can instead be used for mounting the PV cell(s), which are soldered to a custom printed circuit board (PCB). This external connector is then cabled internally to the base hardware in exactly the same way an antenna would be were one installed instead of a PV cell array. This approach minimizes cost, as it requires no retooling of the case or manufacturing process. Figure 6 shows the fully assembled RMSA with lid both open and closed. For this work, the SLMD121H10L PV cell was chosen, for reasons mentioned in the PV cell evaluation section, and two are needed for maximum system lifetime under indoor lighting conditions. Full testing results are presented in the next section.

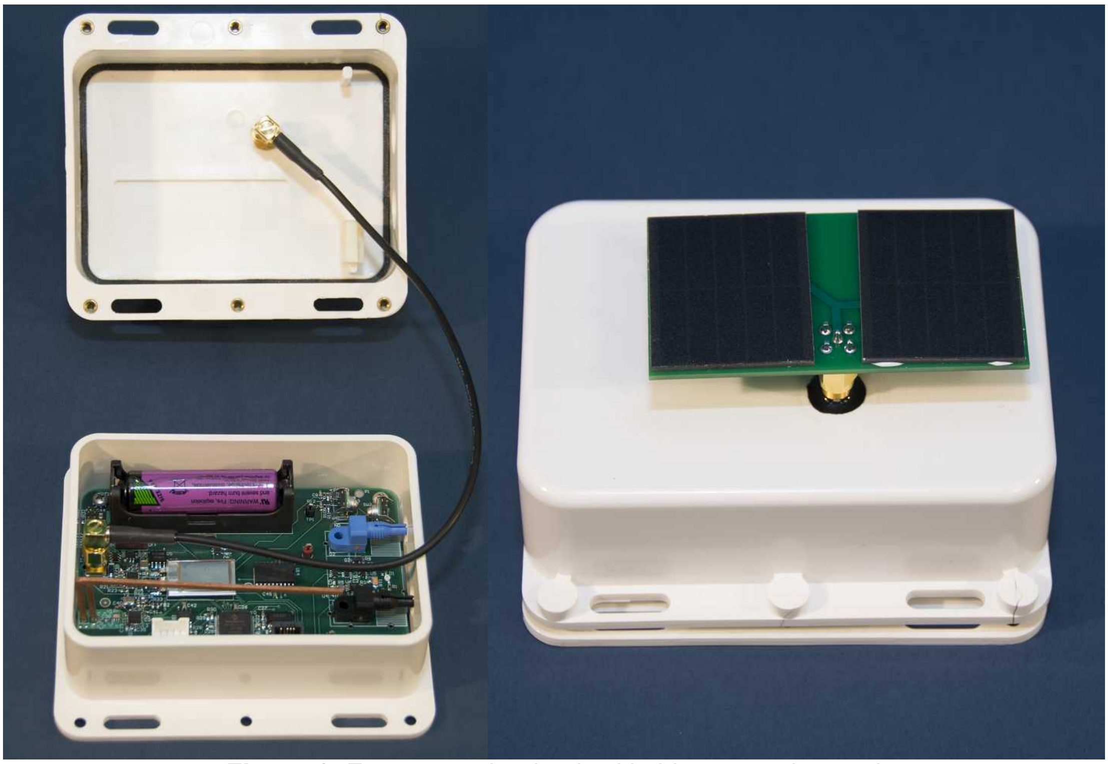

Figure 6: Fully assembled unit with lid open and closed

As previously mentioned, batteries must still be contained within the unit to prevent external tampering and seal power-down. Nevertheless, because ambient PV energy is so abundant, the base hardware in this instantiation only contains one battery rather than the standard two. This reduction offsets the cost of one of the attached SLMD121H10L PV cells. Additionally, because the design is a tiered architecture, a secondary storage unit is included. This unit is carefully sized to match the power needs of the attached system and the lighting cycle. For reasons mentioned in [1], an EDLC supercapacitor is once again the preferred storage medium. Given that RMSA requires a quiescent current of ~20 µA and an operating voltage of 2.5 V – 3.6 V and assuming a typical warehouse environment, with artificial lighting in place for at least 12 hours a day, a fully charged supercapacitor must contain at least 660 mF of capacitance to fully power the system without requiring switchover to the primary battery. The nearest value commercially available is 470 mF, which is used in this design, allowing for 8.6 hours of continuous operation without any available solar energy when fully charged.

For this work, no modification of the RMSA firmware is necessary. However, should further diagnostics be desired, such as the amount of charge on the secondary storage, the hardware connections on the base design require no alteration. Only the firmware would require change, notably to digitize such an analog measurement and then add it to the periodic State-of-Health message.

5. Performance

To measure the performance of the system, three different lighting types were evaluated. The types chosen are representative of what might be present in an indoor environment and include LED, fluorescent, and incandescent. Each type of lighting contains different spectral power distribution curves that characterize the power emitted per wavelength of light.

For each lighting source, the harvester was placed a fixed distance away corresponding to a given illumination level. The illumination level and color of the light was measured using a spectrometer, and the test was repeated four times at different illumination levels. For these tests, light illumination was measured in lux. If watts is preferred, lux may be converted using the following equation

$$P(w) = \frac{E_{V\,(lx)} * A_{(m^2)}}{\eta_{(\frac{lm}{W})}}$$

Where P is the power in watts, E_V is the illuminance in lux, A is the area in square meters, and η is the luminous efficacy in lumens per watt. For typical lighting, η is 15 for tungsten incandescent, 60 for a compact fluorescent, and 30 for a white LED.

The results for each type of lighting are shown below, as is the spectral output of each light type. The Y axis in each figure represents the current harvested by the device in amps, while the X axis is the measured illumination level in lux. The figure also plots the average current required by an RMSA.

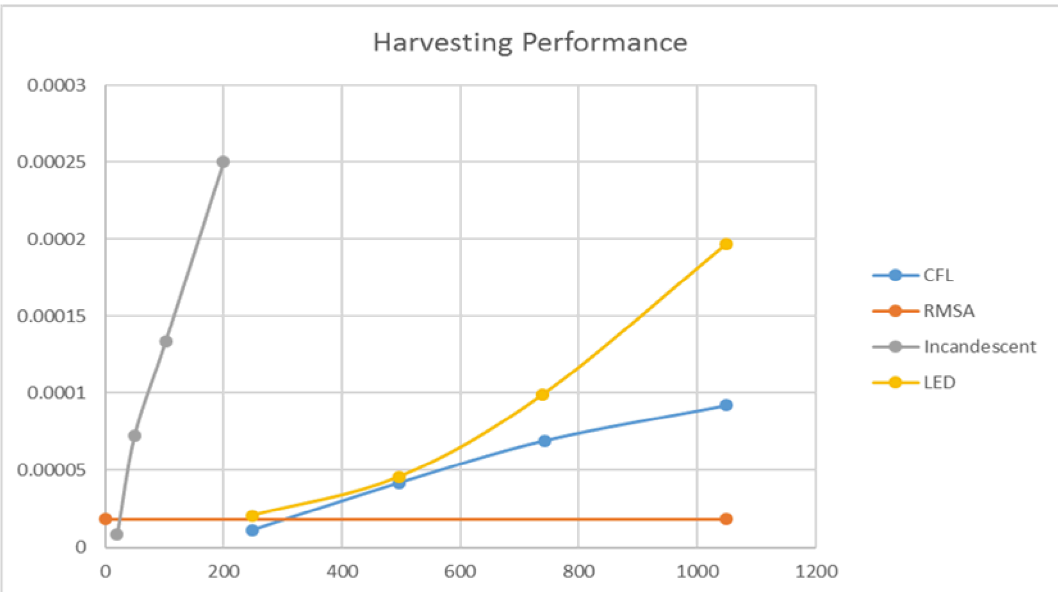

Figure 7: Harvesting Results

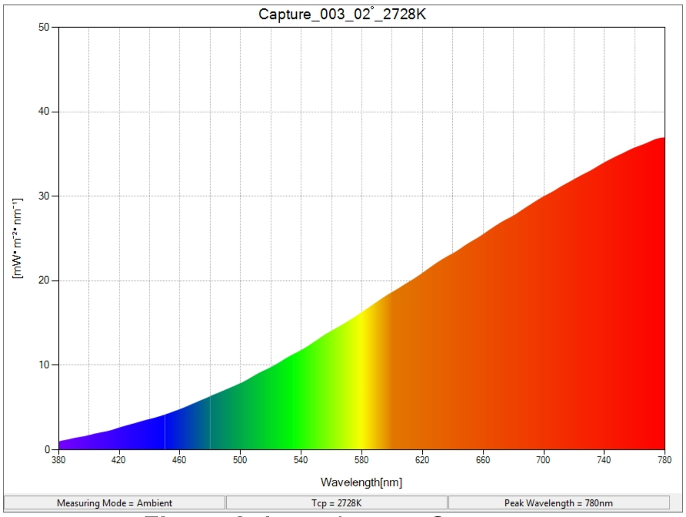

Figure 8: Incandescent Spectrum

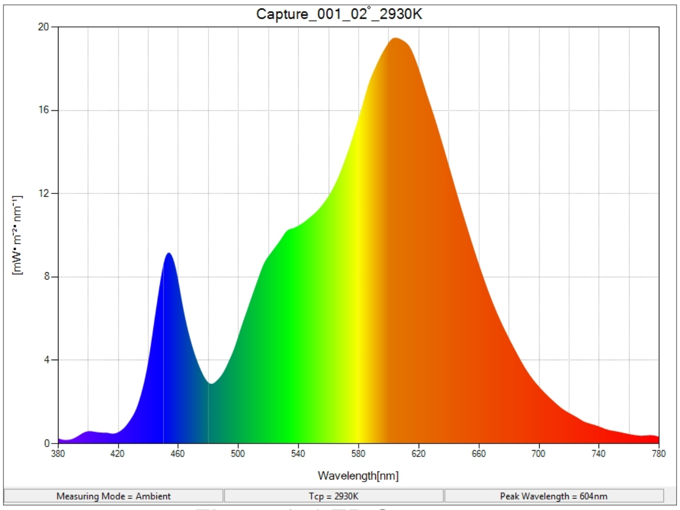

Figure 9: LED Spectrum

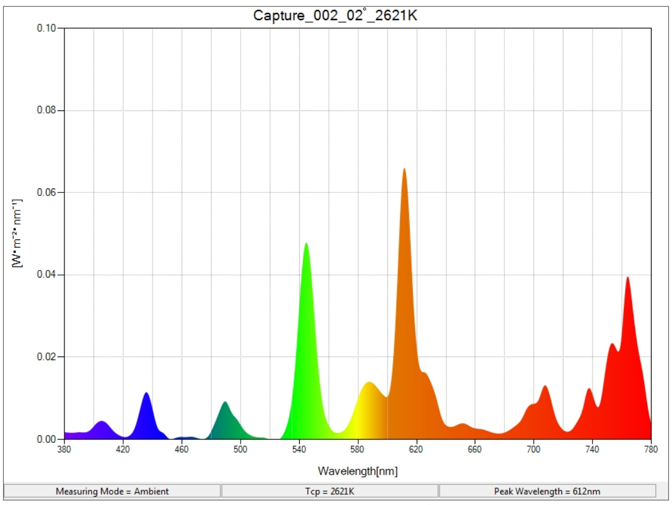

Figure 10: Fluorescent Spectrum

As shown in Figure 7, for illumination levels above ~30 lux for incandescent and ~250 lux for fluorescent/LED, the harvester is able to fully power a single RMSA. Incandescent light is clearly superior, as it provides the whitest output of the three lighting styles resulting in less required illumination. Also, these required illumination levels are low and easily attainable indoors. For reference, in an office with two overhead 40W fluorescent bulbs, the illumination level directly underneath at a distance of seven feet is ~500 lux.

6. Conclusions

There are many different options and architectures available to integrate PV-based energy harvesting with a safeguards instrument, such as a seal. It is up to the designer to match the power requirements of the system to the power available over the course of a lighting cycle. This paper has shown that ~$25 of monocrystalline cells coupled to a $10 PCB assembly can provide enough power, even in sparsely lit indoor areas and regardless of lighting type, to fully power a safeguards instrument, such as RMSA. Further, by using a tiered architecture, this system permits almost 9 hours of downtime within the lighting cycle without still ever having to drain the primary batteries. So long as the cells are not installed in overly dusty or dirty areas, the system will provide self-sustainable operation that is only limited by the lifetime of the electronic components and not the battery.

7. Acknowledgements

The author gratefully acknowledges funding support from the US Department of Energy/National Nuclear Security Administration Safeguards Technology Development Team (NA-241).

Sandia National Laboratories is a multi-mission laboratory managed and operated by National Technology and Engineering Solutions of Sandia, LLC., a wholly owned subsidiary of Honeywell International, Inc., for the U.S. Department of Energy's National Nuclear Security Administration under contract DE-NA0003525.

8. References

[1] Hymel, R; *Far-Field Wireless Energy Harvesting for Increased Safeguards Equipment Battery Life*: Proceedings of the Institute for Nuclear Material Management Annual Conference; 2016.